Activating WASP mutations associated with X-linked neutropenia result in enhanced actin polymerization, altered cytoskeletal responses, and genomic instability in lymphocytes

Lisa S. Westerberg,[1,2,4,7] Parool Meelu,[1,2,4] Marisa Baptista,[7] Michelle A. Eston,[1,2,4] David A. Adamovich,[1,2,4] Vinicius Cotta-de-Almeida,[1,2,4,8] Brian Seed,[3,5] Michael K. Rosen,[9] Peter Vandenberghe,[10,11] Adrian J. Thrasher,[12] Christoph Klein,[13] Frederick W. Alt,[5,6] and Scott B. Snapper[1,2,4]

[1]Gastrointestinal Unit, [2]Center for the Study of Inflammatory Bowel Diseases, and [3]Center for Computational and Integrative Biology, Massachusetts General Hospital, Boston, MA 02114
[4]Department of Medicine, [5]Department of Genetics, and [6]Howard Hughes Medical Institute, Children's Hospital Boston, Immune Disease Institute, Harvard Medical School, Boston, MA 02115
[7]Unit of Clinical Allergy Research, Department of Medicine, Karolinska Institute, Stockholm 17176, Sweden
[8]Oswaldo Cruz Institute, Fundação Oswaldo Cruz, Rio de Janeiro, RJ, 21045-900, Brazil
[9]Howard Hughes Medical Institute and Department of Biochemistry, University of Texas Southwestern Medical Center, Dallas, TX 75390
[10]Center for Human Genetics and [11]Department of Hematology, University Hospital Leuven and University of Leuven, 3000 Leuven, Belgium
[12]Molecular Immunology Unit, UCL Institute of Child Health, University College London, London WC1N 1EH, England, UK
[13]Department of Pediatric Hematology and Oncology, Hannover Medical School, 30625 Hannover, Germany

X-linked neutropenia (XLN) is caused by activating mutations in the Wiskott-Aldrich syndrome protein (WASP) that result in aberrant autoinhibition. Although patients with XLN appear to have only defects in myeloid lineages, we hypothesized that activating mutations of WASP are likely to affect the immune system more broadly. We generated mouse models to assess the role of activating WASP mutations associated with XLN (XLN-WASP) in lymphocytes. XLN-WASP is expressed stably in B and T cells and induces a marked increase in polymerized actin. XLN-WASP–expressing B and T cells migrate toward chemokines but fail to adhere normally. In marked contrast to WASP-deficient cells, XLN-WASP–expressing T cells proliferate normally in response to cell-surface receptor activation. However, XLN-WASP–expressing B cells fail to proliferate and secrete lower amounts of antibodies. Moreover, XLN-WASP expression in lymphocytes results in modestly increased apoptosis associated with increased genomic instability. These data indicate that there are unique requirements for the presence and activation status of WASP in B and T cells and that WASP-activating mutations interfere with lymphocyte cell survival and genomic stability.

CORRESPONDENCE
Scott B. Snapper:
ssnapper@hms.harvard.edu

Abbreviations used: aph, aminoglycoside phosphotransferase; BAC, bacterial artificial chromosome; ES, embryonic stem; FISH, fluorescent in situ hybridization; GST, glutathione S-transferase; WASP, Wiskott-Aldrich syndrome protein; XLN, X-linked neutropenia.

The actin cytoskeleton is essential for proper functioning of the immune system by regulating cell movement, cell–cell interactions, cell signaling, and cell division. The Wiskott-Aldrich syndrome protein (WASP) is uniquely expressed in hematopoietic cells and is a key organizer of cell shape through coordination of receptor signaling to remodeling of the actin cytoskeleton. WASP is critically dependent on its structural conformation and is thought to reside in an inactive form in the cytoplasm caused by an intramolecular interaction between the GTPase binding domain and the C-terminal verprolin-cofilin-acidic domain (Kim et al., 2000). Binding of WASP-interacting proteins such as Cdc42 and Nck can release this autoinhibition, exposing the verprolin-cofilin-acidic domain to the Arp2/3 complex and globular actin, and inducing actin polymerization. WASP deficiency affects the immune system broadly, and WAS patients suffer from immunodeficiency, thrombocytopenia, and

The Rockefeller University Press $30.00
J. Exp. Med. Vol. 207 No. 6 1145-1152
www.jem.org/cgi/doi/10.1084/jem.20091245

The Journal of Experimental Medicine

eczema and are at increased risk to develop autoimmunity and tumors (Notarangelo et al., 2008; Bosticardo et al., 2009). To date, at least 150 loss-of-function mutations in the gene encoding WASP have been identified in WAS patients (Thrasher and Burns, 2010). Three novel mutations (L270P, S272P, and I294T) clustered within the GTPase binding domain of WASP were recently identified in patients with a severe congenital form of X-linked neutropenia (XLN; Devriendt et al., 2001; Ancliff et al., 2006; Beel et al., 2009). The L270P, S272P, and I294T mutations destroy the autoinhibited conformation of WASP and generate an unfolded protein with enhanced actin-polymerizing activity (Devriendt et al., 2001; Ancliff et al., 2006; Beel et al., 2009).

The main features of severe congenital neutropenia are the onset of major bacterial infections early in life, paucity of mature neutrophils, maturation arrest at the promyelocyte/myelocyte stage in the bone marrow, and increased risk of developing leukemia (Dale and Link, 2009). Severe congenital neutropenia is caused by loss-of-function mutations in a variety of proteins including the genes encoding neutrophil elastase, HAX1, and the recently identified glucose-6-phosphatase catalytic subunit 3 (Ancliff, 2003; Klein et al., 2007; Boztug et al., 2009). The XLN-WASP mutations (L270P, S272P, and I294T) add to the genetic complexity of the disease (Devriendt et al., 2001; Ancliff et al., 2006; Beel et al., 2009). Although deficiency in neutrophil elastase, HAX1, and glucose-6-phosphatase catalytic subunit 3 can be explained by increased apoptosis of neutrophils and their precursors, it is difficult to predict how constitutively active WASP may induce neutropenia and how the function of other hematopoietic cells are affected. We have recently provided a mechanism for induction of neutropenia in which forced expression of WASP-I294T in a monocyte cell line induced increased polymerized actin, delayed cell-cycle progression, increased apoptosis, and genomic instability with multinucleated and tetraploid cells (Moulding et al., 2007).

Because WASP deficiency broadly affects all hematopoietic cells, we hypothesized that XLN mutations in WASP may be critical for the function of other hematopoietic cells in addition to neutrophils. In this report, we aimed to clarify the role of WASP-L270P and WASP-I294T in B and T cell function using novel knockin mouse models. We demonstrate that XLN mutations in WASP interferes with normal activation of lymphocytes by inducing a marked increase in polymerized actin, decreased cell spreading, and increased apoptosis associated with increased genomic instability.

RESULTS AND DISCUSSION

WASP-L272P and WASP-I296T induce increased actin polymerization in vitro, and are stably expressed and functional in live cells

We first sought to determine if mouse XLN mutations of WASP, WASP-L272P, and WASP-I296T, corresponding to the human WASP-L270P and WASP-I294T mutations, would lead to increased activation of WASP, and if they are expressed and functional in live cells. To test the activity of WASP-L272P and WASP-I296T in vitro, we used assays to detect actin-polymerizing activity (Cory et al., 2002; Ancliff et al., 2006). Beads coated with WASP-WT, WASP-L272P, and WASP-I296T were used to induce actin polymerization in cell lysates. In this assay, WASP-WT supported little to no actin polymerization (Fig. 1 A, left), supporting the notion that WASP resides as an inactive form in the resting state (Kim et al., 2000). In contrast, WASP-L272P and WASP-I296T induced a marked increase in polymerized actin (Fig. 1 A, middle and right). The increased polymerized actin induced by WASP-L272P and WASP-I296T was confirmed by Western blot analyses (Fig. 1 B). We also confirmed the increased actin-polymerizing activity of the XLN-activating mutation of WASP (WASP-L272P) by pyrene actin assays (unpublished data; Adamovich et al., 2009). To test the expression and functionality of WASP-L272P and WASP-I296T, an infection model was used. N-WASP–deficient fibroblasts fail to support actin tail formation by the vaccinia virus (Fig. 1 C; Snapper et al., 2001). This defect can be rescued by expression of WASP-WT, which localizes to the pole of the actin tail (Fig. 1 C; Snapper et al., 2001). WASP-L272P and WASP-I296T supported actin tail formation by vaccinia in N-WASP–deficient fibroblasts and localized to the pole of actin tails (Fig. 1 C), demonstrating that WASP-L272P and WASP-I296T are expressed and functional in live cells.

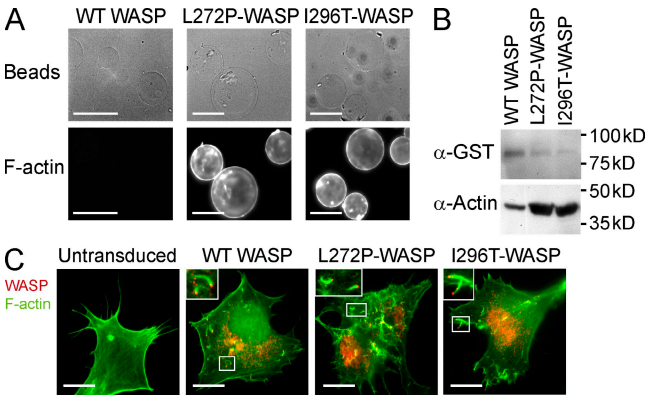

Figure 1. WASP-L272P and WASP-I296T induce increased actin polymerization in vitro, and are stably expressed and functional in live cells. (A and B) In vitro actin-polymerizing assay. GST-WASP fusion proteins were purified with glutathione sepharose beads and incubated with cell lysates to induce actin polymerization. Polymerized actin (F-actin) was visualized on beads after labeling with phalloidin (A) or by Western blotting using anti-actin antibodies (B). Bars, 100 µm. (C) Expression of WASP and rescue of vaccinia actin tail formation. Retrovirions expressing WASP-WT, WASP-L272P, and WASP-I296T with an N-terminal flag tag were used for protein expression in N-WASP–deficient fibroblasts. The cells were subsequently infected with vaccinia virus that forms characteristic actin tails visualized with phalloidin (green). Localization of WASP proteins was determined using anti-flag antibodies (red). Vaccinia fails to form tails in untransduced N-WASP–deficient fibroblasts (left). Insets show higher magnification of boxed areas highlighting vaccinia virus actin tails. Bars, 20 µm. These experiments represent one of at least three independent experiments.

WASP-I296T and WASP-L272P are expressed in B and T cells and induce a marked increase in polymerized actin

To determine the role of activating WASP mutations in hematopoietic cells, we assembled a bacterial artificial chromosome (BAC) containing the activating WASP-I296T mutation that was used to target embryonic stem (ES) cells (Fig. S1 A; Cotta-de-Almeida et al., 2003). Appropriately targeted ES cells were identified by unique restriction enzyme digestion (Fig. S1 B), and confirmed by fluorescent in situ hybridization (FISH) using a WASP probe (Fig. S1 C) and by direct sequencing of the targeted region (Fig. S1 D). To investigate the function of activated WASP mutations in lymphocytes, we used RAG-2–deficient blastocyst complementation with WASP-I296T–targeted ES cells (Chen et al., 1993). Blastocysts from RAG-2–deficient mice implanted into foster mothers generate animals that fail to rearrange antigen receptor genes and consequently lack mature B and T cells. Injection of gene-targeted ES cells into RAG-2–deficient blastocysts leads to the generation of somatic chimeras in which all mature B and T cells derive from the injected ES cells. We found no profound block in development of B and T cell lineage cells in the WASP-I296T mice (unpublished data). WASP-I296T was expressed at similar levels to WASP-WT in lymph node and spleen B and T cells (Fig. 2 A). To assess the actin-polymerizing activity of WASP-I296T in vivo, the quantity of polymerized actin was determined in naive B and T cells. Although WASP-WT and WASP-deficient B and T cells had a similar quantity of polymerized actin, B and T cells expressing WASP-I296T had markedly elevated levels of polymerized actin (Fig. 2 B). We used a complementary gene therapy approach (Klein et al., 2003) and showed that another XLN mutation, WASP-L272P, was expressed in T cells (Fig. S2 A) and induced markedly elevated levels of polymerized actin (Fig. S2 B). These results demonstrate that WASP-L272P and WASP-I296T are stably expressed in lymphocytes and induce markedly increased polymerized actin.

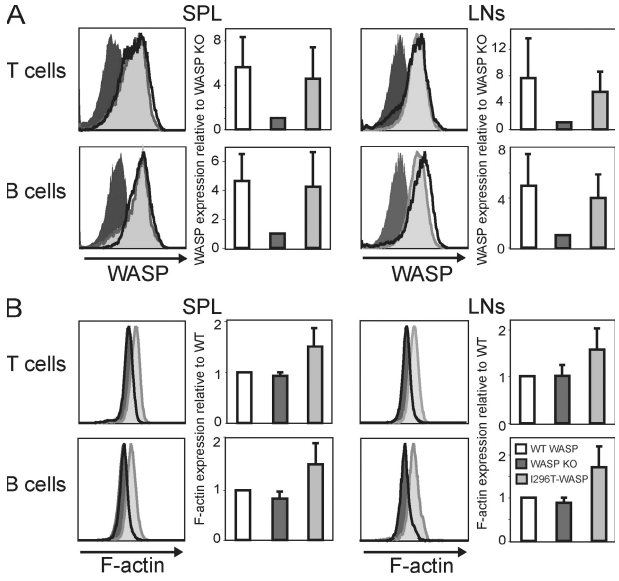

Figure 2. WASP-I296T and WASP-L272P are expressed in B and T cells and induce marked increase in polymerized actin. (A) WASP expression. Spleen and lymph node T and B cells were stained for WASP using an anti-WASP antibody followed by flow cytometric analysis. (B) Polymerized actin (F-actin) content. Spleen and lymph node T and B cells were stained with phalloidin to detect F-actin and analyzed by flow cytometry. Each panel shows one representative histogram (left) and one graph (right) of mean values (±SD) of six experiments ($n = 6$; A) and five experiments ($n = 5$; B).

Normal migratory response but reduced spreading of WASP-L272P and WASP-I296T B and T cells

Because WASP family members play a critical role in cytoskeletal reorganization and correct trafficking of immune cells, we examined receptor-mediated cytoskeletal responses of lymphocytes expressing activating mutations of WASP. An in vitro chemotaxis assay was used to address whether WASP-I296T expression would influence the migration of B and T cells in response to the chemokines CCL19 and CXCL12, which are critical for homing of mature B and T cells into lymphoid organs. The migration of WASP-I296T B and T cells to CXCL12 and CCL19, respectively, was indistinguishable from WT cells (Fig. 3 A), whereas WASP-deficient B and T cells displayed a decreased migratory response, as previously shown (Fig. 3 A; Snapper et al., 2005; Westerberg et al., 2005). To model the contact area between a T cell and an antigen-presenting cell, T cells were incubated on surfaces coated with antibodies to CD3 and CD28 that mimic T cell receptor activation. The T cell receptor–induced and actin-dependent spreading response of both WASP-I296T and WASP-deficient T cells was significantly reduced as compared with WT cells (Fig. 3 B, top; and Fig. 3 C, left). To assess the effect of WASP-I296T on B cell spreading, activated B cells were incubated on surfaces coated with antibodies to CD44. A high percentage of WT B cells formed large protrusions (Fig. 3 B, bottom left), whereas WASP-deficient B cells showed decreased formation of large protrusions, as previously shown (Fig. 3 B, bottom middle; and Fig. 3 C, right; Westerberg et al., 2001). WASP-I296T B cells showed an even more pronounced defect in the formation of long protrusions (Fig. 3 B, bottom right; and Fig. 3 C, right). Notably, although the WASP-I296T B cells failed to form long protrusions, some of the cells formed many short protrusions (Fig. 3 B, right), consistent with aberrant cytoskeletal regulation of cell shape in these cells. We also examined the migratory and spreading response of the additional XLN mutation, WASP-L272P, in B and T cells using the gene therapy model. Similar to the findings with WASP-I296T, the migratory response of WASP-L272P B and T cells was similar to WT cells (Fig. S2 C). The spreading response of WASP-L272P T cells and the formation of long protrusions by WASP-L272P B cells were decreased similarly to the response of WASP-deficient cells (Fig. S2 D).

Decreased surface receptor–induced proliferative responses of WASP-I296T B cells but not T cells

The actin cytoskeleton plays a key role in mitosis and pharmacologically induced actin disorganization leads to growth arrest (Gachet et al., 2001; Ganem and Pellman, 2007). In mice,

we and others have previously shown that WASP is essential for receptor-mediated T cell proliferation, whereas WASP-deficient B cells proliferate normally (Snapper et al., 1998; Zhang et al., 1999; Cotta-de-Almeida et al., 2007). We sought to determine the influence of constitutively active WASP on surface receptor–induced proliferation of lymphocytes. Although WASP-deficient T cells showed nearly completely abolished proliferative responses, WASP-I296T T cells proliferated similarly to WT T cells (Fig. 4 A, left). In contrast, WASP-I296T B cells showed reduced proliferation when compared with both WT and WASP-deficient B cells (Fig. 4 A, left). We addressed whether the decreased proliferative response of WASP-I296T B cells would influence antibody class switch recombination. WT, WASP-deficient, and WASP-I296T B cells were cultured with LPS or IL-4 plus anti-CD40 antibodies to induce switching to IgG2b and IgG1, respectively. As we have previously shown, WASP-deficient B cells showed an increased frequency of IgG2b-, and to a lesser extent, IgG1-switched B cells as compared with WT B cells (Fig. 4, B and C; Westerberg et al., 2005). WASP-I296T cells showed a tendency to decreased class switching as compared with WT B cells, although this difference did not reach significance (Fig. 4, B and C). We next examined antibody secretion and found that WASP-I296T B cells showed a marked reduction in secretion of both IgG2b and IgG1 as compared with WT and

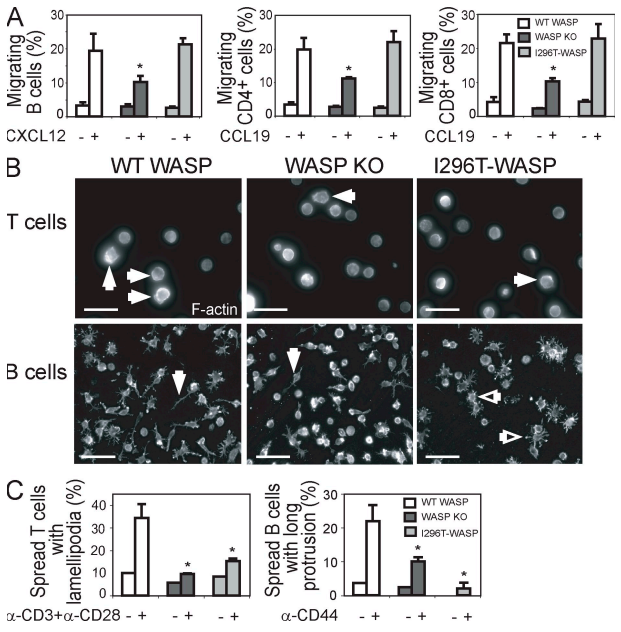

Figure 3. Normal migratory response but reduced spreading of WASP-L272P and WASP-I296T B and T cells. (A) Migration. Spleen B or T cells were allowed to migrate to CXCL12 or CCL19 for 3 h using an in vitro chemotaxis chamber. Migrating cells were collected and enumerated by flow cytometry with reference beads. The percentage of migrating cells is shown as mean values (±SD) of triplicate wells and is representative of at least three experiments. *, $P < 0.05$ compared with WT. (B) Spreading. (top) Spreading of T cells was assessed on anti-CD3 plus anti-CD28 antibody–coated surfaces. Closed white arrows depict the formation of large sheet-like lamellipodia of spread T cells. Bars, 25 µm. (bottom) Spreading of activated B cells was assessed on anti-CD44 antibody–coated surfaces. Closed white arrows depict the formation of long protrusions of spread B cells and open white arrows depict spread cells with many short protrusions. Bars, 40 µm. (C) Graphs show the mean of relative numbers (±SD) of spread T (left) and B cells (right) in triplicates and are representative of three experiments. *, $P < 0.05$ compared with WT.

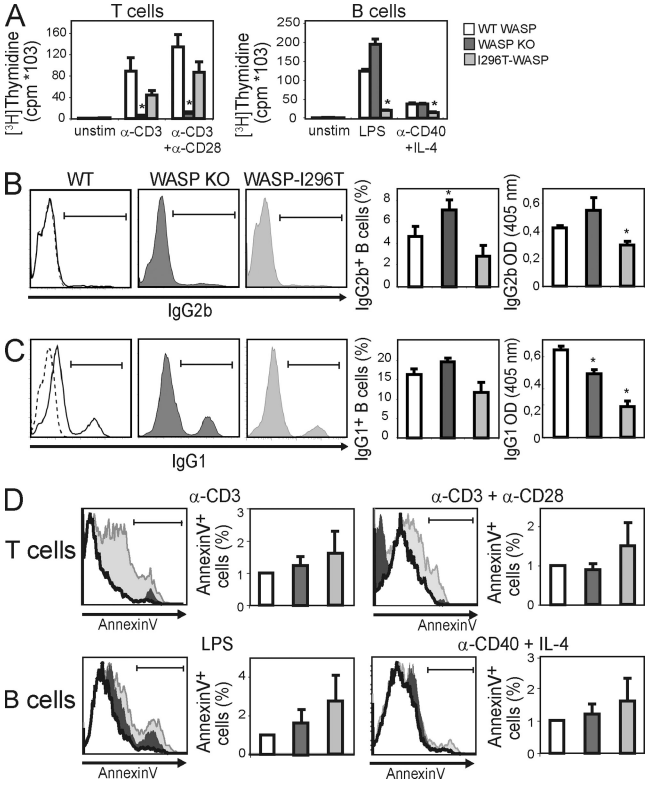

Figure 4. WASP-I296T reduces the proliferative response of B cells, but not T cells, and leads to modestly increased apoptosis. (A) Proliferation. Spleen T (left) and B cells (right) were stimulated for 48 h with the indicated stimulus followed by a 16-h pulse with [^{3}H]thymidine to determine the proliferative response. Bars are representative mean values of cpm ([^{3}H]thymidine) ± SD of triplicate wells from one of at least three independent experiments. *, $P < 0.05$ compared with WT. (B and C) Spleen B cells were stimulated with LPS (B) and anti-CD40 plus IL-4 (C) for 96 h and assessed for IgG2b (B) and IgG1 (C) class switching by intracellular staining and antibody secretion by ELISA. Each panel shows one representative histogram (left) and one graph of mean values (±SD) of three different mice (middle). The dashed lines in the WT histograms (left) indicate the isotype control. Graphs (right) show secretion of IgG2b (B) and IgG1 (C) by ELISA. Each graph represents mean values (±SD) of three different mice. B and C represent one out of two similar experiments. *, $P < 0.05$ compared with WT. (D) Apoptosis. Spleen T and B cells were stimulated with the indicated stimulus for 72 h. The percentage of apoptotic cells was assessed after labeling with 7AAD and annexin V and flow cytometric analysis. Apoptotic cells were defined as annexin V^{high}7AAD^{lo}. Each panel shows one representative histogram (left) and one graph of mean values (±SD) of three or more experiments (right). In each case, although there were statistically significant differences ($P < 0.05$) in apoptosis between WASP-I296T cells when compared with WASP-WT in most individual experiments, because of the variability, statistical significance was not met when compiling all experiments.

WASP-deficient cells (Fig. 4, B and C). These results suggest that B and T cells have different requirements for WASP activity during cell proliferation and that T cells are clearly sensitive to WASP deficiency, whereas B cells are sensitive to constitutive activation of WASP. Moreover, B cells expressing constitutively active WASP have decreased secretion of antibodies.

WASP-I296T induces a modestly increased apoptosis of B and T cells

Bone marrow cells from one WASP-I294T patient demonstrated increased polymerized actin and a greater percentage of apoptotic cells as compared with cells from a healthy individual (Ancliff et al., 2006). Moreover, pharmacologically induced actin polymerization leads to increased apoptosis of monocyte cells (Moulding et al., 2007), suggesting that an increased load of polymerized actin renders cells prone to undergoing apoptosis. We examined whether increased polymerized actin in WASP-I296T lymphocytes was associated with increased apoptosis. Compared with WT and WASP-deficient B and T cells, expression of WASP-I296T led to a modest increase in receptor-induced apoptosis that was greater in B cells than in T cells (Fig. 4 D and Fig. S3).

Increased genomic instability in WASP-I296T B and T cells

Our data indicate that B and T cells expressing WASP-I296T have increased polymerized actin and are prone to apoptosis. These processes are associated with increased genomic instability (Ganem and Pellman, 2007; Moulding et al., 2007). To directly determine a potential role of WASP-I296T in the maintenance of genomic stability, we used a telomere-FISH assay that combines DAPI staining of chromosomes with a telomere-specific peptide nucleic acid probe to assay metaphase chromosomes for chromosomal abnormalities (Zha et al., 2007). WT and WASP-deficient B and WT T cells showed few if any chromosomal aberrations (Fig. 5, top left; and Table I). It was not possible to assess genomic instability in WASP-deficient T cells because they fail to proliferate in response to receptor activation (Fig. 4 A). In contrast, WASP-I296T B and T cells showed increased genomic instability, including chromosome breaks, doublet and fused chromosomes, and tetraploidy (Fig. 5 and Table I). Overall, these findings indicate that WASP activation and its associated cytoskeletal changes alter genomic stability in lymphocytes.

We have used novel mouse models to demonstrate that constitutively active WASP induces increased polymerized actin in B and T cells, and this is associated with decreased spreading, greater apoptosis, and increased genomic instability. Three XLN mutations (L270P, S272P, and I294T) in patients are predicted to destabilize the autoinhibited conformation of WASP and render WASP constitutively active (Devriendt et al., 2001; Ancliff et al., 2006; Beel et al., 2009). Biochemical analysis revealed that WASP-L270P is more rapidly degraded by proteases in vitro than WT WASP (Devriendt et al., 2001). It was previously shown that WASP is expressed in peripheral blood cells from XLN patients (Devriendt et al., 2001). Our results now show that mouse WASP-L272P and WASP-I296T are expressed stably in lymphocytes. Our data support the molecular model for WASP activation in which the open, active conformation of WASP leads to increased polymerized actin. Although regulated polarization of actin is a key feature of T and B cell receptor activation (Batista and Harwood, 2009; Dustin, 2009), little is known about how an increased pool of polymerized actin would influence the function of lymphocytes. We demonstrate that increased polymerized actin is associated with a unique dysfunction of lymphocytes, including decreased cell spreading and increased apoptosis. Two recent papers show that deficiency in coronin1A, a negative regulator of actin dynamics, leads to increased polymerized actin in thymocytes and T cells associated with increased apoptosis (Föger et al., 2006; Shiow et al., 2008). Although coronin1A-deficient thymocytes and T cells have a decreased capacity to migrate to chemokines in vitro and fail to egress normally from the thymus (Föger et al., 2006; Shiow et al., 2008), our results show that WASP-I296T B and T cells migrate normally to chemokines. This indicates that in addition to increased polymerized actin in WASP-I296T B and T cells (which is also appreciated in cononin1A-deficient cells), constitutive activation of WASP

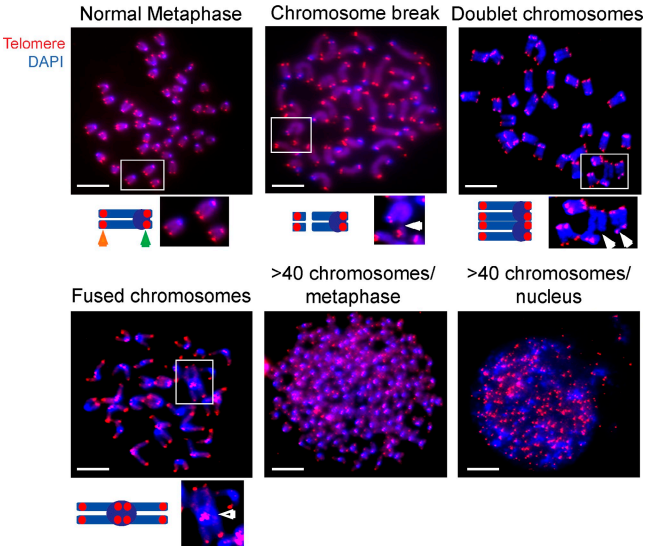

Figure 5. Increased genomic instability in WASP-I296T B and T cells. (A) Examples of cytogenetic abnormalities observed in WASP-I296T B and T cells. DAPI-stained chromosomes are blue, with the centromeres being visualized as more intense blue ovals. Red dots come from telomere signals. The top left micrograph depicts a normal metaphase with 40 chromosomes, each consisting of two sister chromatids and four telomeres. The schematic drawing represents one chromsome with two sister chromatids. The orange arrow denotes telomeres at the long arms and the green arrow denotes telomeres on the short arms of the chromatids. Insets show higher magnification of boxed areas to highlight normal and altered chromosomes. The other micrographs depict representative chromosomal abnormalities including chromosomal breaks (top middle micrograph), doublet chromosomes with breaks (top right micrograph), a fused chromosome (bottom left micrograph), a metaphase with >40 chromosomes (bottom middle micrograph), and a nucleus with >40 chromosomes, i.e., >160 telomeres (bottom right micrograph). Closed white arrowheads in the magnified images beneath the micrographs denote chromosomal breaks. The open white arrowhead denotes two fused chromosomes with a large centromere. Bars, 2 µm.

Table I. Genomic instability in WASP-I296T B and T cells

	Metaphases	Chromosome breaks	>40 chromosomes per metaphase	>40 chromosomes per nucleus	Other
B cells					
WT WASP	51	0	0	0	0
	131	0	0	0	0
	79	0	0	0	0
WASP KO	81	1	0	0	0
	71	0	0	0	0
	54	0	0	2	0
WASP-I296T	160	3	16	1	1 fused chromosome
	73	2	0	4	2 doublet chromosomes
	56	1	0	0	0
T cells					
WT WASP	50	0	0	0	0
	38	0	0	0	0
	72	0	0	0	1 doublet chromosome
WASP-I296T	39	0	0	0	0
	206	17	0	0	1 doublet chromosome
	64	3	1	0	1 doublet chromosome

Quantification of chromosomal aberrations in B and T cells. Each row represents an analysis of cells from one mouse. It was not possible to assess genomic instability in WASP-deficient T cells because they fail to proliferate in response to receptor activation.

may alter unique actin-dependent and/or -independent functions. Collectively, these results add to the complexity of actin cytoskeletal dynamics in lymphocytes in which an increased load of polymerized actin may be as devastating as altered polarization of polymerized actin.

Our results define different requirements for WASP activity in B and T cells with regard to cell proliferation. A hallmark of WASP deficiency in mice is that WASP-deficient T cells fail to respond to T cell receptor activation (Snapper et al., 1998; Zhang et al., 1999; Cotta-de-Almeida et al., 2007). We now show that WASP-I296T–expressing T cells proliferate normally to surface receptor stimulation. In marked contrast, WASP-deficient B cells have normal surface receptor–induced proliferation, whereas WASP-I296T–expressing B cells showed a markedly decreased proliferative response. This demonstrates that B and T cells have different requirements for WASP activity, and that T cells are sensitive to WASP deficiency, whereas B cells are more sensitive to constitutively active WASP. We have previously shown that N-WASP rescues many critical functions of WASP in WASP-deficient thymocytes (Cotta-de-Almeida et al., 2007). N-WASP may not be able to rescue the function of constitutively active WASP if its activity is dominant. In this regard, forced expression of WASP-I294T in a monocyte cell line that expresses WT WASP induces increased polymerized actin, decreased cell-cycle progression, and increased apoptosis, strongly suggesting that constitutively active WASP is dominant over WT WASP activity (Moulding et al., 2007).

Actin is critical during cell division to correctly segregate chromosomes and for cytokinesis by regulating the contractile ring of actin and myosin that cleaves the cell into two daughter cells (Gachet et al., 2001; Ganem and Pellman, 2007). We have previously shown that one WASP-I294T patient had intrinsic defects of myelopoiesis with increased apoptosis in the bone marrow and variable acquired cytogenetic abnormalities (Ancliff et al., 2006). Our results now show that increased polymerized actin in B and T cells expressing WASP-I296T is associated with greater apoptosis and increased genomic instability. It remains to be determined if genomic instability in WASP-I296T hematopoietic cells leads to tumor transformation. This may be a critical issue to consider for the management of XLN patients.

A considerable percentage of severe congenital neutropenia patients have unknown etiology. We predict that some of these patients harbor constitutively active mutations in WASP. In support of this notion, we recently identified the WASP-I294T mutation in a large family with severe congenital neutropenia (Beel et al., 2009). Our data show that mouse XLN mutations of WASP induce a marked increase in polymerized actin in naive B and T cells. Together with our previous results (Westerberg et al., 2005; Ancliff et al., 2006; Moulding et al., 2007), we have determined that increased polymerized actin in hematopoietic cells may be a unique feature of WASP-associated severe congenital neutropenia and can potentially provide a useful screening method to identify new XLN patients.

MATERIALS AND METHODS

Animals. Mice were housed at Children's Hospital Boston and at Massachusetts General Hospital under specific pathogen–free conditions. Animal experiments were performed after approval and in accordance with guidelines from the Subcommittee on Research Animal Care of Children's Hospital Boston and Massachusetts General Hospital.

Generation of DNA constructs and targeted ES cells. The amino acid sequence in the GTPase binding domain spanning the human XLN mutations

of WASP is identical between humans and mice. Based on this sequence identity, we determined that the mouse mutations WASP-L272P and WASP-I296T would correspond to the human XLN mutations WASP-L270P and WASP-I294T, respectively. To generate the glutathione S-transferase (GST)–WASP-WT, WASP-L272P, and WASP-I296T fusion proteins, the WASP cDNA was subcloned into the pEBG vector (a gift from V. Yajnik, Harvard Medical School, Boston, MA), and the L272P (TTG to CCG) and I296T (ATT to ACT) mutations were inserted by site-directed mutagenesis and confirmed by sequencing. The generation of the CMMP-WASP-iresGFP retroviral construct was described previously (Klein et al., 2003), and is now modified by insertion of the L272P and I296T mutations as for the GST constructs. In each retrovirus, a flag tag was inserted 5′ of the ATG start codon of the WASP-WT, WASP-L272P, and WASP-I296T cDNAs to detect WASP protein by immunoflourescence. To assemble the WASP-I296T targeting construct, we used BAC recombineering with some modifications to the previously described method (Cotta-de-Almeida et al., 2003). In brief, 1 kb of genomic WASP spanning exon 9 was cloned into the pSBS171 vector containing an aminoglycoside phosphotransferase (aph) gene cassette flanked by loxP sites and the WASP-I296T mutation was inserted. A 3-kb PCR product encompassing WASP-I296T-loxP-aph-loxP was transformed into bacteria carrying a BAC containing the WASP gene (BACPAC Resources Center at the Children's Hospital Oakland Research Institute). Insertion of WASP-I296T-loxP-aph-loxP into the WASP-containing BAC was performed by homologous recombination mediated by the Red recombination system from bacteriophage λ. The WASP-I296T BAC was linearized with *SgrA1* and used for transfection into J1 ES cells (Yang and Seed, 2003). Two homologous targeted ES cell clones were identified by specific endonuclease digestion using *Dde1*, FISH, and sequencing (Fig. S1, A–D). After deletion of the loxP-aph-loxP cassette by transient expression of the Cre recombinase, two subclones of WASP-I296T ES cells were injected into RAG-2–deficient blastocysts to generate somatic chimeras in which all lymphocytes derive from the WASP-I296T–targeted ES cells (Chen et al., 1993). WT ES cells were injected for RAG-2–deficient blastocyst complementation and used for analysis of WT lymphocytes.

F-actin polymerization assay and vaccinia infection. To determine actin-polymerizing activity, a bead assay was used (Cory et al., 2002). In brief, GST-WASP fusion proteins were purified from lysates of COS-7 epithelial cells with glutathione sepharose 4B beads (GE Healthcare). To induce actin polymerization, WASP-coated beads were incubated with U937 cell lysates in the presence of 5 mM $MgCl_2$. Beads were labeled with Alexa Fluor 488–phalloidin (Invitrogen) to visualize polymerized F-actin by fluorescence microscopy or were boiled in SDS-PAGE loading buffer and analyzed by Western blotting using a monoclonal anti-GST antibody (Santa Cruz Biotechnology, Inc.) to detect GST-WASP fusion proteins and a monoclonal mouse anti-actin antibody (Sigma-Aldrich) to detect actin. For vaccinia rescue assays, N-WASP–deficient fibroblasts were transduced with concentrated retroviruses expressing WASP-WT, WASP-L272P, or WASP-I296T and infected with vaccinia (Snapper et al., 2001). Polymerized actin in vaccinia tails were labeled with Alexa Fluor 488–phalloidin and flag-WASP detected using an anti-flag antibody (Santa Cruz Biotechnology, Inc.) followed by Cy3-conjugated rat anti–mouse secondary antibodies (Jackson ImmunoResearch Laboratories, Inc.).

Flow cytometry. Single-cell suspensions were labeled with fluorescently conjugated anti–mouse antibodies including B220, TCRβ, CD4, and CD8 (eBioscience). For intracellular staining, cells were labeled with purified polyclonal rabbit anti-WASP antibody (a gift from L. Notarangelo, Harvard Medical School, Boston, MA) followed by a donkey anti–rabbit secondary antibody (Jackson ImmunoResearch Laboratories, Inc.) with Alexa Fluor 488–phalloidin to detect polymerized actin or with anti-active caspase-3 (Promega). Data were acquired on a FACSCalibur (BD) and analyzed using FlowJo (Tree Star, Inc.).

In vitro chemotaxis, spreading, proliferation, immunoglobulin detection, and apoptosis. In vitro migration of B and T cells and spreading of B and T cells was assessed as previously described (Westerberg et al., 2001, 2008; Cotta-de-Almeida et al., 2007). For spreading, T cells were incubated on poly–L-lysine–precoated slides, coated with anti-CD3 and anti-CD28 antibodies (eBioscience) for 10 min. B cells were cultured for 48 h in LPS (Sigma-Aldrich) and IL-4 (PeproTech), and incubated on anti-CD44 antibody–coated slides, precoated with poly–L-lysine, for 8 h. Cells were fixed and stained with Alexa Fluor 488–phalloidin. Spread T cells were defined as having a flattened appearance and formation of actin-rich broad lamellipodia as compared with nonspread round cells. Spread B cells were defined as having at least one protrusion longer than one cell diameter in length as compared with nonspread cells. For proliferation, detection of immunoglobulins, and apoptosis, T cells were purified using Dynabeads (Invitrogen) and stimulated with platebound anti-CD3 with or without soluble anti-CD28 stimulating antibodies (eBioscience). B cells were purified with the CellSep B cell enrichment kit (STEMCELL Technologies Inc.) and cultured with LPS or anti-CD40 antibodies (eBioscience) plus IL-4. The proliferative response was assessed as previously described using [^{3}H]thymidine incorporation (Snapper et al., 1998; Cotta-de-Almeida et al., 2007). Antibody class switching and secretion were assessed as previously described using intracellular staining and ELISA for IgG2b and IgG1 (Westerberg et al., 2005, 2008). The frequency of apoptosis was determined as previously described (Cotta-de-Almeida et al., 2007; Westerberg et al., 2008) and apoptotic cells were defined as annexin $V^{high}7AAD^{lo}$ by flow cytometry.

Telomere-FISH. To assess genomic instability, purified B cells were cultured with LPS plus IL-4 and T cells with platebound anti-CD3 and soluble anti-CD28 antibodies for 72 h and prepared for telomere-FISH analysis as previously described (Zha et al., 2007). In brief, cells were treated with the microtubule inhibitor colcemid (Invitrogen) for 5 h to arrest proliferating cells in metaphase. Cells were treated with hypotonic 0.075 M KCl, fixed in MeOH:glacial acetic acid, and dropped on glass slides to generate metaphase spread chromosomes. Telomeres were stained with a Cy3-labeled $(CCCTAA)_3$ peptide nucleic acid probe (Panagene), and DNA was counterstained with DAPI.

Fluorescence microscopy. All slides for fluorescent microscopy were viewed with a research system microscope (Provis AX70; Olympus) using a UplanFl lens at 100× and Mowiol medium (EMD). Images were acquired using a U-PHOTO Universal Photo System camera (U-CMAD-2; Olympus) and were processed with MagnaFire 2.1c (Optronics) and Photoshop CS (version 8.0; Adobe Systems).

Gene therapy model. The gene therapy model was previously described (Klein et al., 2003). In brief, vesicular stomatitis virus-g–pseudotyped retroviruses were generated by transient transfection of CMMPiresGFP-based WASP-WT, WASP-L272P, and empty vector (WASP KO) plasmids into the packaging cell line 293GPG. The supernatant was concentrated and used to infect WASP-deficient $Sca\text{-}1^+lin^-$ progenitor cells at a multiplicity of infection of 10 in the presence of 8 μg/ml polybrene. GFP^+ progenitor cells were injected retroorbitally into lethally irradiated WT recipient mice. Mice were used at week 12 after transplant.

Online supplemental material. Fig. S1 shows the targeting strategy and screening to generate WASP-I296T knockin ES cells. Fig. S2 shows functional analysis of lymphocytes from the XLN-WASP-L272P gene therapy model. Fig. S3 shows detection of apoptotic B and T cells using staining with anti-active caspase-3 antibodies. Online supplemental material is available at http://www.jem.org/cgi/content/full/jem.20091245/DC1.

The authors thank Dr. Y. Fujiwara for blastocyst injections, Dr. V. Yajnik for providing the pEBG vector, and Dr. L. Notarangelo for providing the anti-WASP antibody.

This work was supported by a postdoctoral fellowship from the Wenner-Gren foundation to L.S. Westerberg, by Wellcome Trust grants to A.J. Thrasher, and by National Institutes of Health (NIH) grant HL59561 to S.B. Snapper and United States Immunodeficiency Network–NIH grant AI30070 to L.S. Westerberg and S.B. Snapper. P. Vandenberghe is a senior clinical investigator for Fonds voor Wetenschappelijk Onderzoek–Vlaanderen.

The authors have no conflicting financial interests.

Submitted: 8 June 2009
Accepted: 27 April 2010

REFERENCES

Adamovich, D.A., F. Nakamura, A. Worth, S. Burns, A.J. Thrasher, J.H. Hartwig, and S.B. Snapper. 2009. Activating mutations of N-WASP alter *Shigella* pathogenesis. *Biochem. Biophys. Res. Commun.* 384:284–289. doi:10.1016/j.bbrc.2009.04.050

Ancliff, P.J. 2003. Congenital neutropenia. *Blood Rev.* 17:209–216. doi:10.1016/S0268-960X(03)00019-5

Ancliff, P.J., M.P. Blundell, G.O. Cory, Y. Calle, A. Worth, H. Kempski, S. Burns, G.E. Jones, J. Sinclair, C. Kinnon, et al. 2006. Two novel activating mutations in the Wiskott-Aldrich syndrome protein result in congenital neutropenia. *Blood.* 108:2182–2189. doi:10.1182/blood-2006-01-010249

Batista, F.D., and N.E. Harwood. 2009. The who, how and where of antigen presentation to B cells. *Nat. Rev. Immunol.* 9:15–27. doi:10.1038/nri2454

Beel, K., M.M. Cotter, J. Blatny, J. Bond, G. Lucas, F. Green, V. Vanduppen, D.W. Leung, S. Rooney, O.P. Smith, et al. 2009. A large kindred with X-linked neutropenia with an I294T mutation of the Wiskott-Aldrich syndrome gene. *Br. J. Haematol.* 144:120–126. doi:10.1111/j.1365-2141.2008.07416.x

Bosticardo, M., F. Marangoni, A. Aiuti, A. Villa, and M. Grazia Roncarolo. 2009. Recent advances in understanding the pathophysiology of Wiskott-Aldrich syndrome. *Blood.* 113:6288–6295.

Boztug, K., G. Appaswamy, A. Ashikov, A.A. Schäffer, U. Salzer, J. Diestelhorst, M. Germeshausen, G. Brandes, J. Lee-Gossler, F. Noyan, et al. 2009. A syndrome with congenital neutropenia and mutations in G6PC3. *N. Engl. J. Med.* 360:32–43. doi:10.1056/NEJMoa0805051

Chen, J., R. Lansford, V. Stewart, F. Young, and F.W. Alt. 1993. RAG-2-deficient blastocyst complementation: an assay of gene function in lymphocyte development. *Proc. Natl. Acad. Sci. USA.* 90:4528–4532. doi:10.1073/pnas.90.10.4528

Cory, G.O., R. Garg, R. Cramer, and A.J. Ridley. 2002. Phosphorylation of tyrosine 291 enhances the ability of WASp to stimulate actin polymerization and filopodium formation. *J. Biol. Chem.* 277:45115–45121. doi:10.1074/jbc.M203346200

Cotta-de-Almeida, V., S. Schonhoff, T. Shibata, A. Leiter, and S.B. Snapper. 2003. A new method for rapidly generating gene-targeting vectors by engineering BACs through homologous recombination in bacteria. *Genome Res.* 13:2190–2194. doi:10.1101/gr.1356503

Cotta-de-Almeida, V., L. Westerberg, M.H. Maillard, D. Onaldi, H. Wachtel, P. Meelu, U.I. Chung, R. Xavier, F.W. Alt, and S.B. Snapper. 2007. Wiskott Aldrich syndrome protein (WASP) and N-WASP are critical for T cell development. *Proc. Natl. Acad. Sci. USA.* 104:15424–15429. doi:10.1073/pnas.0706881104

Dale, D.C., and D.C. Link. 2009. The many causes of severe congenital neutropenia. *N. Engl. J. Med.* 360:3–5. doi:10.1056/NEJMp0806821

Devriendt, K., A.S. Kim, G. Mathijs, S.G. Frints, M. Schwartz, J.J. Van Den Oord, G.E. Verhoef, M.A. Boogaerts, J.P. Fryns, D. You, et al. 2001. Constitutively activating mutation in WASP causes X-linked severe congenital neutropenia. *Nat. Genet.* 27:313–317. doi:10.1038/85886

Dustin, M.L. 2009. The cellular context of T cell signaling. *Immunity.* 30:482–492. doi:10.1016/j.immuni.2009.03.010

Föger, N., L. Rangell, D.M. Danilenko, and A.C. Chan. 2006. Requirement for coronin 1 in T lymphocyte trafficking and cellular homeostasis. *Science.* 313:839–842. doi:10.1126/science.1130563

Gachet, Y., S. Tournier, J.B. Millar, and J.S. Hyams. 2001. A MAP kinase-dependent actin checkpoint ensures proper spindle orientation in fission yeast. *Nature.* 412:352–355. doi:10.1038/35085604

Ganem, N.J., and D. Pellman. 2007. Limiting the proliferation of polyploid cells. *Cell.* 131:437–440. doi:10.1016/j.cell.2007.10.024

Kim, A.S., L.T. Kakalis, N. Abdul-Manan, G.A. Liu, and M.K. Rosen. 2000. Autoinhibition and activation mechanisms of the Wiskott-Aldrich syndrome protein. *Nature.* 404:151–158.

Klein, C., D. Nguyen, C.H. Liu, A. Mizoguchi, A.K. Bhan, H. Miki, T. Takenawa, F.S. Rosen, F.W. Alt, R.C. Mulligan, and S.B. Snapper. 2003. Gene therapy for Wiskott-Aldrich syndrome: rescue of T-cell signaling and amelioration of colitis upon transplantation of retrovirally transduced hematopoietic stem cells in mice. *Blood.* 101:2159–2166. doi:10.1182/blood-2002-05-1423

Klein, C., M. Grudzien, G. Appaswamy, M. Germeshausen, I. Sandrock, A.A. Schäffer, C. Rathinam, K. Boztug, B. Schwinzer, N. Rezaei, et al. 2007. HAX1 deficiency causes autosomal recessive severe congenital neutropenia (Kostmann disease). *Nat. Genet.* 39:86–92. doi:10.1038/ng1940

Moulding, D.A., M.P. Blundell, D.G. Spiller, M.R. White, G.O. Cory, Y. Calle, H. Kempski, J. Sinclair, P.J. Ancliff, C. Kinnon, et al. 2007. Unregulated actin polymerization by WASp causes defects of mitosis and cytokinesis in X-linked neutropenia. *J. Exp. Med.* 204:2213–2224. doi:10.1084/jem.20062324

Notarangelo, L.D., C.H. Miao, and H.D. Ochs. 2008. Wiskott-Aldrich syndrome. *Curr. Opin. Hematol.* 15:30–36. doi:10.1097/MOH.0b013e3282f30448

Shiow, L.R., D.W. Roadcap, K. Paris, S.R. Watson, I.L. Grigorova, T. Lebet, J. An, Y. Xu, C.N. Jenne, N. Föger, et al. 2008. The actin regulator coronin 1A is mutant in a thymic egress-deficient mouse strain and in a patient with severe combined immunodeficiency. *Nat. Immunol.* 9:1307–1315. doi:10.1038/ni.1662

Snapper, S.B., F.S. Rosen, E. Mizoguchi, P. Cohen, W. Khan, C.H. Liu, T.L. Hagemann, S.P. Kwan, R. Ferrini, L. Davidson, et al. 1998. Wiskott-Aldrich syndrome protein-deficient mice reveal a role for WASP in T but not B cell activation. *Immunity.* 9:81–91. doi:10.1016/S1074-7613(00)80590-7

Snapper, S.B., F. Takeshima, I. Antón, C.H. Liu, S.M. Thomas, D. Nguyen, D. Dudley, H. Fraser, D. Purich, M. Lopez-Ilasaca, et al. 2001. N-WASP deficiency reveals distinct pathways for cell surface projections and microbial actin-based motility. *Nat. Cell Biol.* 3:897–904. doi:10.1038/ncb1001-897

Snapper, S.B., P. Meelu, D. Nguyen, B.M. Stockton, P. Bozza, F.W. Alt, F.S. Rosen, U.H. von Andrian, and C. Klein. 2005. WASP deficiency leads to global defects of directed leukocyte migration in vitro and in vivo. *J. Leukoc. Biol.* 77:993–998. doi:10.1189/jlb.0804444

Thrasher, A.J., and S.O. Burns. 2010. WASP: a key immunological multitasker. *Nat. Rev. Immunol.* 10:182–192. doi:10.1038/nri2724

Westerberg, L., G. Greicius, S.B. Snapper, P. Aspenström, and E. Severinson. 2001. Cdc42, Rac1, and the Wiskott-Aldrich syndrome protein are involved in the cytoskeletal regulation of B lymphocytes. *Blood.* 98:1086–1094. doi:10.1182/blood.V98.4.1086

Westerberg, L., M. Larsson, S.J. Hardy, C. Fernández, A.J. Thrasher, and E. Severinson. 2005. Wiskott-Aldrich syndrome protein deficiency leads to reduced B-cell adhesion, migration, and homing, and a delayed humoral immune response. *Blood.* 105:1144–1152. doi:10.1182/blood-2004-03-1003

Westerberg, L.S., M.A. de la Fuente, F. Wermeling, H.D. Ochs, M.C. Karlsson, S.B. Snapper, and L.D. Notarangelo. 2008. WASP confers selective advantage for specific hematopoietic cell populations and serves a unique role in marginal zone B-cell homeostasis and function. *Blood.* 112:4139–4147. doi:10.1182/blood-2008-02-140715

Yang, Y., and B. Seed. 2003. Site-specific gene targeting in mouse embryonic stem cells with intact bacterial artificial chromosomes. *Nat. Biotechnol.* 21:447–451. doi:10.1038/nbt803

Zha, S., F.W. Alt, H.L. Cheng, J.W. Brush, and G. Li. 2007. Defective DNA repair and increased genomic instability in Cernunnos-XLF-deficient murine ES cells. *Proc. Natl. Acad. Sci. USA.* 104:4518–4523. doi:10.1073/pnas.0611734104

Zhang, J., A. Shehabeldin, L.A. da Cruz, J. Butler, A.K. Somani, M. McGavin, I. Kozieradzki, A.O. dos Santos, A. Nagy, S. Grinstein, et al. 1999. Antigen receptor-induced activation and cytoskeletal rearrangement are impaired in Wiskott-Aldrich syndrome protein-deficient lymphocytes. *J. Exp. Med.* 190:1329–1342. doi:10.1084/jem.190.9.1329